FACULTY OF INFORMATION TECHNOLOGY AND ELECTRICAL ENGINEERING

Toni Kuosmanen

The effect of visual detail on cybersickness: Predicting symptom severity using spatial velocity

Bachelor's Thesis
Degree Programme in Computer Science and Engineering
April 2019

Kuosmanen T. (2019) The effect of visual detail on cybersickness: Predicting symptom severity using spatial velocity. University of Oulu, Degree Programme in Computer Science and Engineering. Bachelor's thesis, 39 p.

ABSTRACT

In this work we examine the effect of visual realism on the severity of cybersickness symptoms experienced by users of virtual environments. We also seek to validate a metric called spatial velocity as a predictor of cybersickness. The proposed metric combines the visual complexity of a virtual scene with the amount of movement within the scene.

To achieve this, we prepared two virtual scenes depicting the same environment with a variable level of detail. We recruited volunteers who were exposed to both scenes in two separate sessions. We obtained the sickness ratings after both sessions and saved the data required for spatial velocity calculations.

After comparing the sickness ratings between the two scenes, we found no evidence of the visual realism playing any significant role in the generation of cybersickness symptoms. The spatial velocity also proved inadequate in characterizing the difference in visual complexity and correlated poorly with all the observed sickness scores.

Keywords: cybersickness, visually induced motion sickness, head-mounted displays, spatial velocity

Kuosmanen T. (2019) Visuaalisen yksityiskohtaisuuden vaikutus VR-pahoinvointiin: Oireiden vakavuuden ennustaminen käyttäen SV-metriikkaa. Oulun yliopisto, tietotekniikan tutkinto-ohjelma. Kandidaatintyö, 39 s.

TIIVISTELMÄ

Tässä työssä tutkimme sitä, millainen vaikutus virtuaalisten ympäristöjen graafisella yksityiskohtaisuudella on VR-pahoinvointiin. Pyrimme myös validoimaan "spatial velocity"nimisen mittasuureen kyvyn ennustaa VR-pahoinvoinnin oireiden vakavuutta. Kyseisen mittasuureen etuna on, että se yhdistää visuaalisen kompleksisuuden ja ympäristössä koetun liikkeen yhdeksi suureeksi.

Tutkimusta varten valmistimme kaksi virtuaaliympäristöä, joissa mallinnettiin Oulun yliopiston kampusaluetta. Toinen ympäristö pyrki mahdollisimman realistiseen esitystapaan, kun taas toisessa yksityiskohtien määrä minimoitiin. Koetta varten värväsimme 18 vapaaehtoista. Vapaaehtoiset altistettiin kummallekin ympäristölle kahdessa noin kymmenen minuutin mittaisessa kokeessa. Vapaaehtoisten kokeman VR-pahoinvoinnin vakavuutta arvioitiin kunkin kokeen jälkeen täytetyillä kyselylomakkeilla. Kokeiden aikana tallensimme myös SV laskentaan tarvittavat tiedot.

Verrattuamme koeolosuhteiden tuloksia, emme löytäneet todisteita siitä, että ympäristön graafisten yksityiskohtien määrällä olisi merkittävää vaikutusta koettuun pahoinvointiin. Käytetty SV metriikka ei myöskään kyennyt erottelemaan ympäristöjä oletetulla tavalla, eivätkä lasketut arvot korreloineet merkittävästi minkään mitatun pahoinvointisuureen kanssa.

Avainsanat: cybersickness, visually induced motion sickness, head-mounted displays, spatial velocity

TABLE OF CONTENTS

ABBREVIATIONS

CoG	center of gravity
FMS	fast motions sickness scale
HD/LD	high detail / low detail
HMD	head mounted display
IMU	Inertial Measurement Unit
MSSQ	motion sickness susceptibility questionnaire
SSQ	simulator sickness questionnaire
SF	spatial frequency
SV	spatial velocity
VE	virtual environment
VR	virtual reality

1. INTRODUCTION

Virtual reality systems have been around since the 1980s. These systems are characterized by high level of presence, or the illusion being a part of the depicted environment. This high level of presence is achieved by vividly rendering the environments through technologies like head mounted displays and through the use of natural interactions [1].

Over the years, virtual reality systems have found a wide range of applications. Militaries have been early adopters of VR systems, utilizing them for flight simulators and pilot training. For example, The Super Cockpit project, headed by Thomas Furness, produced an HMD based system that could project live flight data to pilots [2, 3].

Virtual reality has also been utilized in other areas of training, ranging from new employee orientation at Walmart to teaching job critical skills to professionals. For example, it was shown by Seymour et al. that training surgeons in virtual environments can clearly increase operating room performance [4, 5].

Perhaps the most significant development in recent years is the development and proliferation of affordable VR based consumer entertainment systems. With multiple competing manufacturers, including Oculus Rift, HTC Vive and others, VR based systems now have more users than ever. Analysts are predicting that over six million VR devices will be shipped globally in the year 2019 [6].

One aspect that has slowed the widespread adoption of VR systems is the fact that some users experience a set of symptom collectively referred to as cybersickness. Closely related to motion sickness, the symptoms of cybersickness include feelings of nausea, disorientation, and oculomotor disturbances. The symptoms can last for long after the exposure, even for days in some cases [7].

The likelihood of cybersickness symptoms varies depending on the type of system used. An older study, conducted in 1994 by Regan and Price, found that 61% of the 146 test participants displayed some symptoms after a 20 minute exposure while 5% of the participants suffered symptoms so severe that they had to drop out of the experiment [8, 9]. A more recent study by Kim et al. made similar findings, with almost 80% of the reporting symptoms after just 9.5 minutes of exposure [10].

Previously, it was hoped that in time the causes of cybersickness could be alleviated through the progress of related technologies. The opposite has proven true, however, with the increasing availability of VR capable devices moving the problem affecting fighter pilots and other professionals to the general public [11]. The devices used to render the virtual environments are becoming more powerful each year enabling the creation of scenes of increasing visual quality. How this improvement in visual quality and realism affects the onset of cybersickness is a little studied aspect of cybersickness research. A study from 2001 by Jaeger et al, utilizing static and dynamic walking simulators, compared two scenes of varying visual detail depicting a hallway. The other scene was richly textured while the other featured only gradient lines. They observed that the pre and post-exposure SSQ score differential was on average higher for subjects viewing the high detail scenes, although the difference was not found to be statistically significant [12]. Pouke et al. got similar results while comparing two VR scenes created with the Unreal game engine [13]. The high detail scene strived for maximum visual realism while the other scene utilized cell shading postprocessing to

produce a much less complex visual look. The subjects immersed in the high detail scenes displayed higher average SSQ scores and peak FMS values.

Since the likelihood and severity of cybersickness are strongly dependent on the used scenes and devices, researchers have found it difficult to compare the results of different cybersickness studies. To remedy this, So et al. proposed a new metric, called spatial velocity, to quantify the aspects of virtual environments they suspected to be the leading causes of cybersickness [14]. The proposed metric combines the visual complexity of the virtual scene with the amount of scene movement to get a better measure of the total amount of visual stimuli experienced by the subject. Calculation of spatial velocity requires that scene movement speeds and a steady stream of screenshots are captured from the scene under examination. The metric then combines the velocities and the level of detail, calculated as the dominating spatial frequency of each row and column of the captured screenshots, into a set of measures in all six movement directions. The study found strong correlation between movements in the fore-aft and yaw directions and the total SSQ scores of the test subjects. Further, it was proposed that SV values could be used to calculate the cybersickness dose value.

In this work, we aim to further examine the effects of visual realism on cybersickness. We study this by comparing the symptom scores from two virtual scenes of differing level of detail. We also seek to validate the spatial velocity metric as a indicator of cybersickness. The increased visual complexity of the high detail scene should manifest as higher spatial velocity values and also lead to more severe cybersickness symptoms.

2. BACKGROUND

2.1. Symptoms of cybersickness

Cybersickness is closely related to motion sickness. The conditions differ in the fact that onset of motion sickness symptoms are usually accompanied by the stimulation of the vestibular system while cybersickness symptoms can be activated purely by visual stimuli. [7]

Cybersickness, like motion sickness, presents a wide range of symptoms. In cybersickness research the symptoms are often separated into three categories: nausea, oculomotor and disorientation. The most common symptoms are listed in table 1.

Table 1. Cybersickness symptom categories

Nausea	Oculomotor	Disorientation
Stomach awareness	Eyestrain	Dizziness
Increased salivation	Difficulty focusing	Vertigo
Burping	Blurred vision	
Nausea	Headache	

These categories trace back to the work done by Kennedy et al on the simulator sickness questionnaire [15]. This work, which focused on military flight simulations, found that the symptom profile of simulator sickness was distinct from the profile exhibited by motion sickness, with oculomotor being the dominating symptom cluster [16]. Later it was shown by Stanney et al that the symptoms reported by users of virtual environments differed from those reported by simulator users [17]. Disorientation was found to be the predominant symptom cluster for VE users and the total severity was also estimated as three times higher. This discovery in part led to cybersickness being recognized as a distinct ailment.

It has been shown that frequent use of virtual environments lead to habituation and a decrease in the severity of the symptoms. For example, in a study conducted by Howarth et al it was found that after ten trial sessions half of the test subjects displayed no symptoms after exposure [18]. Even though habituation can decrease the symptoms, potential users of VR systems will most likely find the idea of suffering through habituation period unappealing.

2.2. Theories of cybersickness

2.2.1. Sensory mismatch

The sensory mismatch theory states, that motion sickness is caused when conflicting information is received from the sensory systems [19]. This conflict can occur between information received from different sensory systems or within a single sensory system. The brain doesn't know how to handle the conflicting information which triggers the symptoms related to motion sickness.

In the case of virtual environments, the most probable source of sensory mismatch is vection. Vection is traditionally defined as the illusion of motion caused by visual stimulus [20]. A classical example of vection is that of a passenger sitting aboard a stationary train, watching another train roll by. Even though the passengers train remains motionless, the passenger might feel as if her own train has started moving. Vection in itself does not necessarily cause cybersickness. Keshavarz et al. found in their review that although visually induced motion sickness is generally accompanied by vection, the opposite does not hold true [21]. They reason that since the human vestibular system responds to changes in velocity (i.e. accelerations and decelerations), vection induced by linear movement at a constant speed does not cause severe sensory mismatch.

Display lag and tracking errors also been sources of sensory mismatch, especially in HMD based VR systems. These limitations used to be based on hardware, but with modern HMD setups both tracking performance and latency have been greatly improved [7, 11]. Still, care should be taken when designing VR systems in order to translate the tracked body movements to the VE as naturally as possible. Unnatural compensation of body movements can increase the sensory mismatch and thus cybersickness symptoms. For example, Palmisano et al. showed that a VR scene where the head movements of the test subjects were inversely compensated (i.e. the rotations in the yaw axis were reversed) produced much higher cybersickness ratings [22]. Compared to the inversely compensated case, the normally compensated and uncompensated modes produced 70 % less severe cybersickness ratings.

2.2.2. Postural instability

The postural instability theory, proposed by Riccio et al., states that motion sickness is not caused by sensory mismatch but rather by the prolonged inability to maintain a stable posture [23]. In the context of cybersickness, postural instability manifests in the form of altered specificity [7]. This means that the learned patterns and behaviors of maintaining a stable posture do not work when engaged in virtual environments. For example, if a subject visually perceives a rotation along the fore-aft axis, he might instinctively try to correct his posture by tilting his body in the opposite direction. Since the rotation is not real, the corrective move only produces postural instability. If the instability persists, the symptoms will grow worse. Eventually the subject can learn new patterns of behavior to maintain postural stability in the VE, which explains the decrease of symptom severity through habituation.

2.2.3. Evolutionary theories

The evolutionary significance of motion sickness has been pondered upon by researchers. The physiological responses induced by motion sickness, such as vomiting, seem peculiar and counter productive to the survival of the individual. And yet humans and other primates and mammals are susceptible to motion sickness [24].

An interesting theory to explain the nausea associated with motion sickness was proposed by M. Treisman in 1977. The so called poison theory proposes that the other

symptoms associated with motions sickness are similar to those caused by ingesting certain neurotoxins. The body responds to the symptoms by trying to purge the poison by vomiting. [25]

An alternative theory was proposed by Bowins [26]. The negative reinforcement model proposes that the negative symptoms occur to teach the organism to avoid movements and situations that cause postural instability or unexpected movements which in turn helps to reduce the risk of injury. The theory helps to explain the fact that motion sickness is rarely observed in infants and toddlers. Since toddlers and infants do not possess physical capabilities for avoiding the situations causing motion sickness, the negative reinforcement system has not been yet developed.

2.3. Measuring cybersickness

2.3.1. Simulator sickness questionnaire

The most common method of measuring cybersickness symptoms is the simulator sickness questionnaire (SSQ). Originally developed in 1993 by Kennedy et al. for evaluating military flight simulators, the questionnaire is still widely used in cybersickness research [16].

The questionnaire contains 16 different symptoms that are divided into three categories: oculomotor, disorientation and nausea. Some symptoms contribute to multiple categories. The symptoms included in the questionnaire and the categories they belong to are listed in table 2. The questionnaire is usually administered after exposure, but sometimes the questionnaire is also filled before the the exposure and the difference in scores is reported. However, this is not recommended in the original article and it has been shown that the the practice tends to inflate the sickness ratings [27].

When filling the questionnaire, the subjects are asked to rate how strongly they are experiencing each of the 16 symptoms on a four point scale. The scores for the three categories and a total score can then be obtained using the following formulas:

$$SSQ_N = \sum S_N * 9{,}54 \tag{1}$$

$$SSQ_O = \sum S_O * 7{,}58 \tag{2}$$

$$SSQ_D = \sum S_D * 13{,}92 \tag{3}$$

$$SSQ_T = \sum S * 3{,}74 \tag{4}$$

SSQ_N, SSQ_O, and SSQ_D refer to nausea, oculomotor, and disorientation sub scores respectively while SSQ_T is the total score. The scores don't have an absolute scale, which means that the SSQ values of individual applications should be interpreted in the context of similar applications.

Table 2. SSQ symptom clusters

Symptom	N	O	D
General discomfort	X	X	
Fatigue		X	
Headache		X	
Eye strain		X	
Difficulty focusing		X	X
Increased salivation	X		
Sweating	X		
Nausea	X		X
Difficulty concentrating	X	X	
Fullness of head			X
Blurred vision		X	X
Dizziness (eyes open)			X
Dizziness (eyes closed)			X
Vertigo			X
Stomach awareness	X		
Burping	X		

2.3.2. Other subjective measures

Fast motion sickness scale

Fast motion sickness scale (FMS) offers an alternative way for monitoring cybersickness symptoms. During VE exposure, the subjects are asked to rate their feelings of nausea on a 20 point scale, at one minute intervals. This results in a time profile of the sickness symptoms which might be useful in identifying nausea inducing sections of the VE under examination. The peak and mean scores correlate well with both nausea and total SSQ scores. However, since only the nausea ratings are measured and symptoms related to cybersickness ignored, FMS might not be sufficient to fully characterize the negative effects of a particular VE. [28].

Motion sickness susceptibility questionnaire

The motion sickness susceptibility questionnaire (MSSQ), developed by Reason and Brand [19], is often administered along with SSQ. The original questionnaire was later improved by Golding [29]. Since individual susceptibility to cybersickness varies greatly, test results, especially with smaller populations, can become skewed. Scores obtained from MSSQ can be used to partially factor these effects of individual variations out. The questionnaire is divided into two parts, with the first section focusing on childhood experiences with motion sickness and the second part concerned with experiences in recent years.

2.3.3. Measuring postural instability

Since the postural instability theory states that the inability to maintain a stable posture is the sole cause of motion sickness, many methods have been developed to measure the instability. Traditionally, these methods can be roughly divided in two two categories: static and dynamic methods. In static methods the subject is asked to stay in some slightly challenging posture, like standing on one foot with eyes closed, for a set amount of time. The amount of time the subject manages to maintain this position is then measured. In dynamic methods the subject is asked to complete some simple task, such as walking in a straight line with eyes closed. The number of successfully performed actions or the number of failures can then be counted to obtain an estimate of postural stability. Since the boundary between successfully holding a posture or completing an action and a failure is vague, both methods suffer from low precision [30].

Recently, posturographic methods, where the postural stability is estimated with the help of some external measuring device, such as a balance board, have been gaining in popularity. For example Chardonnet et al. examined the the sway area of the center of gravity (CoG) using a high end balance board [31]. Their results showed, that as the subjects started to suffer from cybersickness symptoms, the CoG area of sway increased and changed shape, transforming from an ellipse to a more circular shape. Examining the results further in the frequency domain revealed an increase in higher frequency (2-3 Hz range) movements in both fore-back and left-right directions. These higher frequency movements are usually associated with involuntary movements caused by the loss of balance.

Since most VR systems come equipped with a wide range of gyroscopes and acceleration sensors, it seems feasible that postural instability could be identified directly from the device sensor output. However, to our knowledge no such work has yet been attempted.

2.3.4. Biometric measurements

Biometric measurements provide an alternative objective measure of of cybersickness. Earlier research in motion sickness has shown that the symptoms are associated with readily measurable physiological changes, such as gastric tachyarrhythmia, increase skin conductance and changes in heart rate or brain activity [32, 33, 34].

Several attempts have been made to discover good predictors of cybersickness, although the results have been mixed. Kim et al. examined 16 different electrophysiological signals during a 9.5 minute exposure to multi screen VR system and compared the results with SSQ scores [35]. Examination of the data revealed that any single variable showed only weak correlations to the SSQ scores, however, they managed to build a multi variable regression model, including that could predict 46 % of the variation in the severity of cybersickness. Also, they discovered, rather anomalously, that the heart period of their subjects correlated positively with the sickness ratings. This is unusual since feelings of nausea are usually associated with increased heart rate.

More recently, Dennison et al. performed a similar examination of physiological measurements. They too were unable to find a a single variable that could explain the

variation in symptom severity but were likewise able to build multivariable regression model [36]. They had particular success with the SSQ-O scores, where their model could explain 74.7 % of the variance. The study also featured two different viewing conditions, with each subject viewing the environment through normal display monitors before experiencing the same environment using an OculusRift HMD. They were able to confirm that the physiological responses between the two viewing conditions were different. Utilizing linear discriminant analysis, they were able to predict with 77.8 % accuracy which viewing condition the data under examination belonged to.

3. RESEARCH METHODS

3.1. Setup

To study the effects of visual realism on cybersickness, we used two scenes featuring the campus area of Oulu University. The scenes were identical in their scale and geometry but the other scene aimed for high visual realism while the other utilized a shading technique that drastically reduced the level of detail. A comparison shot of the two scenes is shown in figure 1. Both scenes were constructed using Unreal Engine version 4.19.2. Oculus Rift was used to view the scenes.

Figure 1. A comparison shot featuring a view from the University lobby between the high (a) and low (b) detail scenes.

To equalize the amount of VE exposure in both test conditions, we prepared a static route along which the user agent would be transported during testing. The path was fixed in length and duration in both scenes, with user agents traveling at constant speed. The duration of the route was approximately ten minutes. Although movement within the scene was limited to the path, the camera angle was not restricted and the users were able to look around freely.

Spatial velocity calculations require that spatial and angular velocities are recorded. For this purpose, we developed a simple logging component for the Unreal Engine. The component writes the current timestamp, user agent's position, camera rotation, and the approximate frame rate at regular intervals to a log file. During the experiments, a sampling rate of 5 Hz was used.

At the request of our research partners, we also included raw inertial measurement unit (IMU) data from the HMD device. This IMU data was collected in the hopes that it could be used to identify postural sway related to cybersickness.

3.2. Test procedure

In order to limit the effect of individual variation of cybersickness susceptibility, we decided that each test subject would complete both the high detail (HD) and low detail (LD) test conditions. To eliminate any carry over effects between the experiments, each subject waited at least one week before completing the the other condition. The order of the conditions was randomized.

In total, 22 test subjects were recruited for the experiment. Out of these 18 managed to complete both test conditions. Four subjects had to be dropped due to time constraints. During testing, two subjects, 8 and 9, had to abort the experiment because they became too sick to continue. Their data is still included because 8 almost completed both test conditions and 9 successfully completed the LD condition.

Before starting the first experiment, each participant filled a background information survey and a shortened version of the MSSQ[1]. Informed consent was also acquired from each participant. To facilitate future research, we also collected supplemental biometric data. The chest strapped heart rate monitor and fitness wristband used to gather this biometric data were also attached during this phase. The data from these two devices was collected using a custom made smart phone application. Before beginning the actual experiment, the participants were asked to perform a sharp hand movement so that the collected sensor data could be synchronized afterwards.

When the pretest surveys were completed, the participants put on the HMD and were given help making adjustments to the unit if necessary. A short explanation of the FMS scoring system was given and the experiment was then started. The logging component was set up so that the data collection began immediately after the user agent starts moving on the preplanned route. FMS ratings were gathered during the experiment at one-minute intervals. All the experiments were recorded using Nvidia ShadowPlay so that the screenshots required for spatial velocity calculations could be extracted later.

After completing the route, the HMD was removed and finally the SSQ was administered. The procedure was the same for the second session. Subjects that managed to complete both test conditions were compensated with free movie tickets. All the data collected during the experiments is summarized in table 3.

[1]MSSQ-Short, see: [37]

Table 3. Collected data

Survey data	Note
Background information	Age, sex, education , eyesight, VR-device use
MSSQ	
FMS	
SSQ	
Log data and video	
Timestamp	ISO-8601
Position	Scene coordinates (x,y,z)
Camera angle	Roll, pitch yaw
View direction	Front and up vectors
HMD IMU data	Linear and angular velocities and accelerations
FPS	
Video	720p resolution @ 24 fps
Biometric sensors	
Heart rate	Chest strapped heart rate monitor
Motion etc.	Activity bracelet

4. RESULTS AND ANALYSIS

4.1. Data processing

To process the results, a simple python script was written. The script takes as input the log file written during the experiment and the recorded video file. The script outputs the player centered velocities, angular velocities, spatial frequencies and the spatial velocities, calculated according to the method described by So et al. [14].

4.1.1. Player centered velocities and angular velocities

The scene velocities [unit/s] were first calculated using the positional data recorded in the log file. The instantaneous velocity was estimated as the positional displacement between two consecutive log rows divided by the time difference. The scene velocities were calculated separately in all the directions. The scene velocities were then transferred to the player centered coordinate system (Figure 2) using the following formula:

$$\boldsymbol{\nu} = \boldsymbol{Q}\boldsymbol{\nu}' \Leftrightarrow \boldsymbol{\nu}' = \boldsymbol{Q}^T\boldsymbol{\nu} \tag{5}$$

In the formula, $\boldsymbol{\nu}$ and $\boldsymbol{\nu}'$ are the world and player centered velocities respectively and $\boldsymbol{Q}$ is the 3x3 orthogonal transformation matrix. When the directions of all the coordinate axes in both coordinate systems $\boldsymbol{x}$ and $\boldsymbol{x}'$ is known, the values of Q can be solved using equation 6:

$$\boldsymbol{Q} = \begin{bmatrix} cos(x_1, x_1') & cos(x_1, x_2') & cos(x_1, x_3') \\ cos(x_2, x_1') & cos(x_2, x_2') & cos(x_2, x_3') \\ cos(x_3, x_1') & cos(x_3, x_2') & cos(x_3, x_3') \end{bmatrix} = \begin{bmatrix} \hat{x}_1 \cdot \hat{x}_1' & \hat{x}_1 \cdot \hat{x}_2' & \hat{x}_1 \cdot \hat{x}_3' \\ \hat{x}_2 \cdot \hat{x}_1' & \hat{x}_2 \cdot \hat{x}_2' & \hat{x}_2 \cdot \hat{x}_3' \\ \hat{x}_3 \cdot \hat{x}_1' & \hat{x}_3 \cdot \hat{x}_2' & \hat{x}_3 \cdot \hat{x}_3' \end{bmatrix} \tag{6}$$

where $\hat{x}_i, \hat{x}_j'$ are the unit vectors of each coordinate axis. Finally, after performing the transformation, the RMS values of all the velocities were saved.

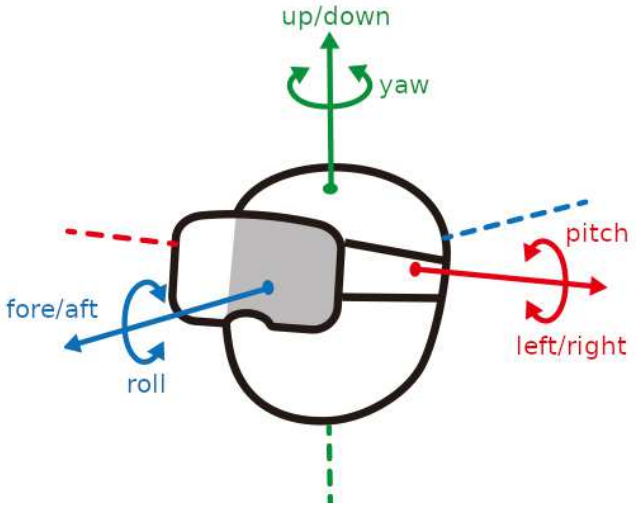

Figure 2. The six degrees of freedom in the player centered coordinate system.

The angular velocities [°/s] were obtained in a similar fashion. The camera rotations were recorded in the log file and the angular velocities calculated from the displacement between two consecutive log items.

All calculated velocities can be found in appendices 1 and 2. The highest velocities were found in the fore-aft direction while the highest angular velocities were on the yaw axis.

4.1.2. Spatial frequencies

The video files recorded during the experiments were used to calculate the spatial frequencies. The videos were loaded using the Python implementation of the OpenCV library [38] and grayscale screenshots were extracted at a steady rate. Each video was sampled at a rate of 2.5 Hz, starting from the point where the user begins to move.

After extracting the screenshots, the dominating spatial frequency of each image was calculated. The method described by So et al. proposes three different ways of choosing the dominant spatial frequency: mean, mode and combined. After some initial testing, the mean method was chosen since the other two showed very little variation between images. First, an estimate of the power spectral density (PSD) of the 1D Fourier transforms of each image row and column was obtained using the SciPy implementation of Welch's method [39, 40]. The mean frequency of the PSD was then chosen as the dominant SF of the current row or column. Finally, the average row and column SF values were calculated. Hann window function and FFT length of 256 was used for all calculations. The radial SF was calculated from the average row and column SF values using the following formula:

$$SF_{rad} = \sqrt{SF_{row}^2 + SF_{col}^2} \tag{7}$$

Figure 3 shows an example calculated row PSD values of a single image. As can be seen from the figure, the SF values were heavily concentrated to the lower frequencies. The calculated spatial frequencies can be found in appendix 3. Surprisingly, the average SF values were found to be generally higher in the low detail scene.

4.1.3. Spatial Velocities

The spatial velocities were calculated as described in the original article by So et al. The SV values are calculated for all six degrees of freedom separately, using the player centered or angular velocities and the average SF values. The formulas for all the SV values are listed in table 4.

The calculated velocities can be found in appendix 4. The highest spatial velocities were found in the fore-aft, horizontal, and yaw directions. As could be predicted from the SF values, the average spatial velocities were higher in the low detail scene.

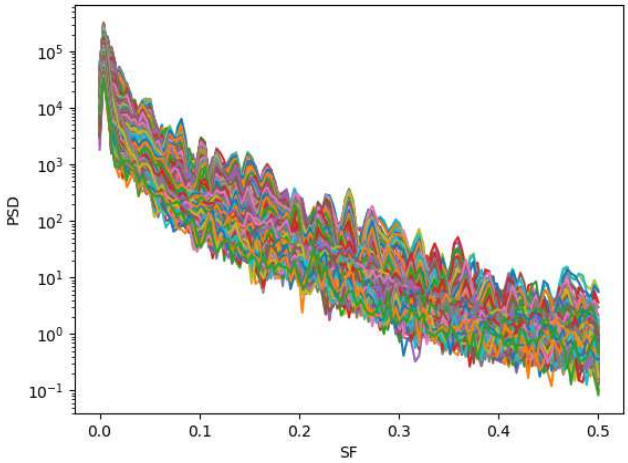

Figure 3. An example of row PSD values calculated for a single image. Each color represents a different row.

Table 4. Spatial velocity formulas

SV Value	Formula	Note
SV_x	$SF_{rad} * V_x$	Fore-aft direction
SV_y	$SF_{row} * V_y$	Left-right
SV_z	$SF_{col} * V_z$	Up-down
SV_{roll}	$SF_{rad} * V_{roll}$	Roll
SV_{yaw}	$SF_{row} * V_{yaw}$	Yaw
SV_{pitch}	$SF_{col} * V_{pitch}$	Pitch

4.1.4. Questionnaires and other data

All the questionnaires were processed by Tapio Kursula as part of his bachelor's thesis. Only the relevant questionnaire data is included in this work. The SSQ scores and peak FMS values can be found in appendix 5.

4.2. Effects of scene detail

The effects of scene detail were analyzed by comparing the measured SSQ scores and peak FMS values between the two scenes. The results of this analysis are presented in table 5. In the table, the Δ is the average in-subject difference in the measures between the test conditions. The difference is almost zero for all the measured sickness ratings. Also displayed in the table is the p-values obtained from single factor ANOVA test for each of the measured ratings.

Table 5. Results of scene detail effect analysis.

Measure	Avg. Δ	ANOVA p-value
SSQ N	2	0.87
SSQ O	-4	0.62
SSQ D	-8	0.64
SSQ T	-3	0.80
Peak FMS	0	0.74

Both the calculated average differences and the results of the ANOVA-test indicate that there is no observable difference in the sickness ratings between the two test conditions.

4.3. Spatial Velocity and the sickness ratings

The connection between the spatial velocities and the sickness ratings was examined by calculating the Pearson's correlation coefficient between each pairing of spatial velocity and sickness measure. The correlations are shown in table 6.

Table 6. Correlations between the sickness measures and spatial velocities

	SSQ_N	SSQ_O	SSQ_D	SSQ_T	FMS_{peak}
SV_{rad}	0.17	0.09	0.02	0.11	0.09
SV_{hor}	-0.30	-0.19	-0.11	-0.23	-0.30
SV_{vert}	0.03	0.06	0.13	0.08	0.06
SV_{roll}	-0.03	-0.05	0.14	0.03	-0.08
SV_{pitch}	-0.05	-0.01	0.22	0.06	-0.09
SV_{yaw}	-0.24	-0.15	-0.01	-0.15	-0.26

As can be seen from the table, no significant correlations exist between the spatial velocities and the sickness measures. The strongest link found between the variables seems to be the slight negative correlations between the horizontal spatial velocity and nausea scores.

5. DISCUSSION

The results of the experiment seem to speak against the level of detail in the virtual scene having any significant effect in the generation of cybersickness effects. Although our sample size was too small to be statistically significant, the average differences between the two conditions were practically zero. On the other hand, it might be the case that the two scenes were simply not different enough. While the surface textures were greatly simplified in the low detail scene, the scene still contained advanced lighting and shading effects. An even more toned down version of the low detail could be constructed, stripping object representations down to the bare minimum. Although most modern VR applications tend to strive for high rather than low level of detail and visual realism, a repeated experiment using very low detail scene might give useful information about the features and patterns that can cause cybersickness.

The use of spatial frequency as a measure of visual complexity proved problematic. Spatial frequency has been widely used in the study of human visual system [41]. Simple patterns, like sine gratings or striped optokinetic drums and the way they generate vection can be characterized using spatial frequency [42]. However, in the analysis of more complex images, the spatial frequency might not be as suitable. The spectral power density in natural images is heavily concentrated to the lower frequencies, with power being inversely proportional to the squared frequency in most cases [43]. This became apparent during the analysis of the results when the dominant spatial frequencies were calculated. The dominant frequencies did not differ much between the high and low detail scenes. Counterintuitively, the higher average spatial frequencies were found in the low detail scenes where the average radial SF was 0.031 compared to 0.026 in the high detail scene. This could mean that spatial frequency is not an adequate measure for quantifying the difference in level of detail.

The analysis of the FMS scores revealed one interesting trend relating to the type of motion most likely to cause feelings of nausea. The route taken by the subjects through the virtual scene was mostly flat but contained short section during the 9 - 10 minute period where the subjects first descended and then ascended a set of stairs. We noticed during testing that many subjects became noticeably ill after this section. This observation was confirmed when the average FMS values were calculated. Figure 4 shows the average FMS values during the test. The descent-ascent period can be seen in the plot as a sharp increase in the average FMS score after the nine minute mark. Earlier experiments have also given signs that vertical movements are provocative [13]. Neither the peak FMS or any of the SSQ scores correlated with the vertical spatial velocity but this might be due to the fact that because the period of vertical movement was so short, the average vertical spatial velocity was low. This presents another problem with the spatial velocity metric: since established measures of cybersickness give only sparse scores, it can be hard to make connections between the features observed in the continuous spatial velocity profile and the observed sickness ratings. Spatial velocities aside, it could be interesting design an experiment to find out what type of movements are most likely to cause cybersickness symptoms.

Overall, we found little evidence to support the use of spatial velocity as a predictor of cybersickness. The correlations between the observed sickness ratings and the spatial velocity scores were all insignificant. Our calculations showed that spatial frequency might be ill suited for characterizing complex images like the high resolution

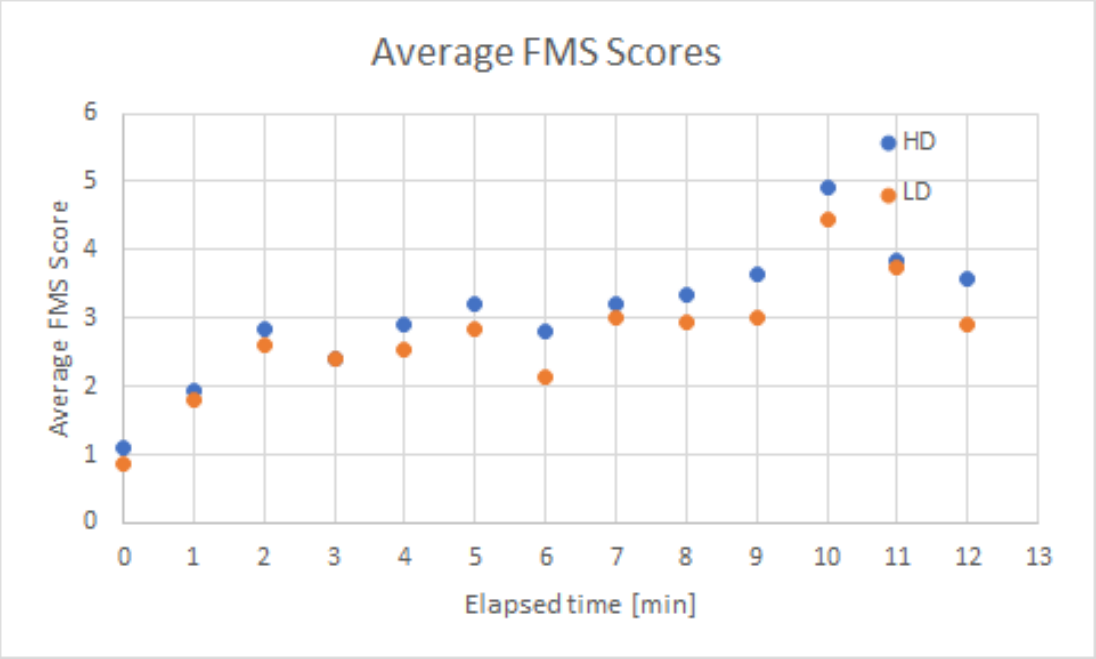

Figure 4. Average FMS scores during testing.

screenshots captured from the videos. Furthermore, based on our results the level of detail has no significant effect on the severity of the symptoms, which makes the whole SF component of spatial velocity redundant. Spatial velocity also requires extensive calculations and logging of data which makes it unwieldy and precludes it's use as a general tool for characterizing virtual scenes.

6. CONCLUSION

In this work, we set out to discover whether the level of visual detail and realism has any effect on the severity of cybersickness symptoms. We also wanted to evaluate the suitability of the spatial velocity metric as a predictor of cybersickness. For this purpose, we prepared two virtual scenes of variable level of detail. Our comparison between the two scenes showed that the level of detail had a negligible effect on all the measured symptoms.

The usefulness of the spatial velocity metric was disputed when our calculations revealed that the average SV values did not correlate well with any of the symptom measures. The spatial frequency component seems to be inadequate in quantifying the difference in level of detail in complex virtual scenes since frequency content in natural images tends to concentrate on the lower frequencies.

We observed a noticeable increase in the average FMS scores during the part of the test when the subjects were going up or down a set of stairs. This suggests that some types of motion are more provocative than others and further research should be done to determine the types of motion most likely to cause severe symptoms.

Another possible avenue of future research is the utilization of the IMU data from the HMD unit that was recorded during the experiment. A predictor of cybersickness symptoms derived from this data would be useful since practically all modern HMD units are equipped with these types of sensors to enable head tracking.

7. REFERENCES

[1] Steuer J. (1992) Defining virtual reality: Dimensions determining telepresence. Journal of communication 42, pp. 73–93.

[2] Lowood H.E. (2018), Virtual reality. URL: https://www.britannica.com/technology/virtual-reality.

[3] Furness III T.A. (1986) The super cockpit and its human factors challenges. In: Proceedings of the Human Factors Society Annual Meeting, vol. 30, SAGE Publications Sage CA: Los Angeles, CA, vol. 30, pp. 48–52.

[4] Gagliordi N. (accessed 2.4.2019), Walmart deploys 17,000 oculus go headsets to train its employees. https://www.zdnet.com. URL: https://www.zdnet.com/article/walmart-deploys-17000-oculus-go-headsets-to-train-its-employees/.

[5] Seymour N.E., Gallagher A.G., Roman S.A., O'brien M.K., Bansal V.K., Andersen D.K. & Satava R.M. (2002) Virtual reality training improves operating room performance: results of a randomized, double-blinded study. Annals of surgery 236, p. 458.

[6] Tsai J. (accessed 10.1.2019), The state of immersive reality in 2018. TrendForce (online). URL: https://press.trendforce.com/press/20181210-3188.html.

[7] LaViola Jr J.J. (2000) A discussion of cybersickness in virtual environments. ACM SIGCHI Bulletin 32, pp. 47–56.

[8] Barrett J. (2004) Side effects of virtual environments: A review of the literature. Tech. rep., DEFENCE SCIENCE AND TECHNOLOGY ORGANISATION CANBERRA (AUSTRALIA).

[9] Regan E. (1994) Some side-effects of immersion virtual reality. AGARD, Virtual Interfaces: Research and Applications 8 p(SEE N 94-37261 12-53) .

[10] Kim Y.Y., Kim H.J., Kim E.N., Ko H.D. & Kim H.T. (2005) Characteristic changes in the physiological components of cybersickness. Psychophysiology 42, pp. 616–625.

[11] Rebenitsch L. & Owen C. (2016) Review on cybersickness in applications and visual displays. Virtual Reality 20, pp. 101–125.

[12] Jaeger B.K. & Mourant R.R. (2001) Comparison of simulator sickness using static and dynamic walking simulators. In: Proceedings of the Human Factors and Ergonomics Society Annual Meeting, vol. 45, SAGE Publications Sage CA: Los Angeles, CA, vol. 45, pp. 1896–1900.

[13] Pouke M., Tiiro A., LaValle S.M. & Ojala T. (2018) Effects of visual realism and moving detail on cybersickness. In: 2018 IEEE Conference on Virtual Reality and 3D User Interfaces (VR), pp. 665–666.

[14] So R.H., Ho A. & Lo W. (2001) A metric to quantify virtual scene movement for the study of cybersickness: Definition, implementation, and verification. Presence: Teleoperators & Virtual Environments 10, pp. 193–215.

[15] Kennedy R.S., Lane N.E., Berbaum K.S. & Lilienthal M.G. (1993) Simulator sickness questionnaire: An enhanced method for quantifying simulator sickness. The international journal of aviation psychology 3, pp. 203–220.

[16] Kennedy R.S. & Fowlkes J.E. (1992) Simulator sickness is polygenic and polysymptomatic: Implications for research. The International Journal of Aviation Psychology 2, pp. 23–38.

[17] Stanney K.M., Kennedy R.S. & Drexler J.M. (1997) Cybersickness is not simulator sickness. In: Proceedings of the Human Factors and Ergonomics Society annual meeting, vol. 41, SAGE Publications Sage CA: Los Angeles, CA, vol. 41, pp. 1138–1142.

[18] Howarth P.A. & Hodder S.G. (2008) Characteristics of habituation to motion in a virtual environment. Displays 29, pp. 117 – 123. URL: http://www.sciencedirect.com/science/article/pii/S0141938207000960, health and Safety Aspects of Visual Displays.

[19] Reason J.T. & Brand J.J. (1975) Motion sickness. Academic press.

[20] Palmisano S., Allison R.S., Schira M.M. & Barry R.J. (2015) Future challenges for vection research: definitions, functional significance, measures, and neural bases. Frontiers in Psychology 6, p. 193. URL: https://www.frontiersin.org/article/10.3389/fpsyg.2015.00193.

[21] Keshavarz B., Riecke B.E., Hettinger L.J. & Campos J.L. (2015) Vection and visually induced motion sickness: how are they related? Frontiers in Psychology 6, p. 472. URL: https://www.frontiersin.org/article/10.3389/fpsyg.2015.00472.

[22] Palmisano S., Mursic R. & Kim J. (2017) Vection and cybersickness generated by head-and-display motion in the oculus rift. Displays 46, pp. 1 – 8. URL: http://www.sciencedirect.com/science/article/pii/S0141938216300713.

[23] Riccio G.E. & Stoffregen T.A. (1991) An ecological theory of motion sickness and postural instability. Ecological Psychology 3, pp. 195–240. URL: https://doi.org/10.1207/s15326969eco0303_2.

[24] MED P.P.I.N.F. (1990) The susceptibility of rhesus monkeys to motion sickness. Aviation, space, and environmental medicine , p. 807.

[25] Treisman M. (1977) Motion sickness: an evolutionary hypothesis. Science 197, pp. 493–495.

[26] Bowins B. (2010) Motion sickness: A negative reinforcement model. Brain Research Bulletin 81, pp. 7 – 11. URL: http://www.sciencedirect.com/science/article/pii/S0361923009003153.

[27] Young S.D., Adelstein B.D. & Ellis S.R. (2006) Demand characteristics of a questionnaire used to assess motion sickness in a virtual environment. In: null, IEEE, pp. 97–102.

[28] Keshavarz B. & Hecht H. (2011) Validating an efficient method to quantify motion sickness. Human factors 53, pp. 415–426.

[29] Golding J.F. (1998) Motion sickness susceptibility questionnaire revised and its relationship to other forms of sickness. Brain Research Bulletin 47, pp. 507 – 516. URL: http://www.sciencedirect.com/science/article/pii/S0361923098000914.

[30] Cobb S.V.G. (1999) Measurement of postural stability before and after immersion in a virtual environment. Applied Ergonomics 30, pp. 47 – 57. URL: http://www.sciencedirect.com/science/article/pii/S0003687098000386.

[31] Chardonnet J.R., Mirzaei M.A. & Merienne F. (2015) Visually induced motion sickness estimation and prediction in virtual reality using frequency components analysis of postural sway signal. In: International Conference on Artificial Reality and Telexistence Eurographics Symposium on Virtual Environments, pp. 9–16.

[32] Cowings P.S., Suter S., Toscano W.B., Kamiya J. & Naifeh K. (1986) General autonomic components of motion sickness. Psychophysiology 23, pp. 542–551.

[33] Hu S., Grant W.F., Stern R.M. & Koch K.L. (1991) Motion sickness severity and physiological correlates during repeated exposures to a rotating optokinetic drum. Aviation, space, and environmental medicine .

[34] Chelen W., Kabrisky M. & Rogers S. (1993) Spectral analysis of the electroencephalographic response to motion sickness. Aviation, space, and environmental medicine 64, pp. 24–29.

[35] Kim Y.Y., Kim H.J., Kim E.N., Ko H.D. & Kim H.T. (2005) Characteristic changes in the physiological components of cybersickness. Psychophysiology 42, pp. 616–625. URL: https://onlinelibrary.wiley.com/doi/abs/10.1111/j.1469-8986.2005.00349.x.

[36] Dennison M.S., Wisti A.Z. & D'Zmura M. (2016) Use of physiological signals to predict cybersickness. Displays 44, pp. 42 – 52. URL: http://www.sciencedirect.com/science/article/pii/S0141938216301081, contains Special Issue Articles – Proceedings of the 4th Symposium on Liquid Crystal Photonics (SLCP 2015).

[37] Golding J.F. (2006) Predicting individual differences in motion sickness susceptibility by questionnaire. Personality and Individual Differences 41, pp. 237 – 248. URL: http://www.sciencedirect.com/science/article/pii/S0191886906000602.

[38] Bradski G. (2000) The OpenCV Library. Dr. Dobb's Journal of Software Tools .

[39] Welch P. (1967) The use of fast fourier transform for the estimation of power spectra: a method based on time averaging over short, modified periodograms. IEEE Transactions on audio and electroacoustics 15, pp. 70–73.

[40] Jones E., Oliphant T., Peterson P. et al. (2001–), SciPy: Open source scientific tools for Python. URL: `https://docs.scipy.org/doc/scipy-0.14.0/reference/generated/scipy.signal.welch.html`, [Online; accessed 7.3.2019].

[41] Shapley R. & Lennie P. (1985) Spatial frequency analysis in the visual system. Annual review of neuroscience 8, pp. 547–581.

[42] Hu S., Davis M.S., Klose A.H., Zabinsky E.M., Meux S.P., Jacobsen H.A., Westfall J.M. & Gruber M.B. (1997) Effects of spatial frequency of a vertically striped rotating drum on vection-induced motion sickness. Aviation, space, and environmental medicine 68, pp. 306–311.

[43] Simoncelli E.P. & Olshausen B.A. (2001) Natural image statistics and neural representation. Annual review of neuroscience 24, pp. 1193–1216.

APPENDIX 1.

1.1. Scene velocities (HD)

		ν_{rad}		ν_{hor}		ν_{ver}	
ID	N	AVG	STD	AVG	STD	AVG	STD
0	1923	171.0	22.5	36.5	35.1	10.1	13.3
1	1923	167.8	25.7	39.0	39.2	15.8	21.7
2	1923	176.1	15.4	17.5	22.4	17.9	14.0
3	1923	161.4	31.0	46.0	47.0	32.3	15.1
6	1923	165.4	26.5	48.6	43.2	14.3	10.3
7	1923	132.0	53.9	89.0	60.5	14.1	22.1
8	1717	156.1	42.0	49.8	50.2	24.3	28.5
9	647	177.5	5.6	19.7	12.9	17.9	6.5
10	1923	178.4	13.7	12.0	14.4	13.3	7.2
12	1923	175.1	13.4	14.7	13.3	36.1	6.7
13	1923	147.1	41.8	73.0	52.4	28.2	18.3
14	1923	163.4	38.4	40.3	49.8	10.5	14.5
15	1923	166.4	24.6	45.9	39.1	18.2	17.9
16	1923	153.1	36.0	65.0	51.2	26.9	16.4
17	1923	174.3	18.2	26.2	29.4	14.6	11.5
18	1923	141.8	44.5	72.5	54.8	32.7	34.5
19	1652	162.7	31.9	45.2	42.0	20.3	28.7

1.2. Scene velocities (LD)

		ν_{rad}		ν_{hor}		ν_{ver}	
ID	N	AVG	STD	AVG	STD	AVG	STD
0	1923	176.6	14.7	22.7	20.7	13.4	7.7
1	1923	173.1	20.4	26.0	32.5	13.9	16.7
2	1792	170.7	24.3	19.2	26.9	35.5	22.6
3	1923	164.6	31.5	42.5	45.7	20.5	14.2
6	1923	158.7	32.7	59.1	48.7	17.9	12.1
7	1923	138.6	49.1	82.8	56.8	18.6	22.6
8	1413	155.5	40.7	57.5	54.1	13.8	15.8
9	1923	177.1	13.4	9.2	7.2	29.3	8.5
10	1923	168.0	26.4	42.1	40.0	10.4	14.1
12	1923	176.6	13.4	9.5	9.1	31.6	6.4
13	1923	135.3	47.1	89.9	54.7	24.8	19.3
14	1923	165.8	32.8	39.6	46.2	12.1	13.4
15	1923	168.3	24.3	41.5	37.9	18.7	13.4
16	1923	156.8	37.2	53.6	53.0	27.1	13.8
17	1923	175.9	16.7	21.0	24.6	15.1	10.0
18	1923	133.6	49.3	84.1	58.3	31.7	29.1
19	1923	163.4	33.8	48.3	45.3	12.1	14.6

APPENDIX 2.

2.1. Scene angular velocities velocities (HD)

		ν_{roll}		ν_{pitch}		ν_{yaw}	
ID	N	AVG	STD	AVG	STD	AVG	STD
0	1923	1.4	2.0	2.7	5.0	26.0	151.9
1	1923	2.5	4.0	5.6	9.4	25.5	140.1
2	1923	1.5	2.0	3.3	6.1	16.0	121.5
3	1923	2.7	4.3	3.2	5.4	23.4	128.9
6	1923	2.2	3.0	2.7	4.4	32.3	159.8
7	1923	4.0	7.5	6.2	11.3	53.6	206.5
8	1717	6.9	28.3	6.4	11.9	47.6	218.1
9	647	1.7	3.2	2.8	4.5	15.9	121.3
10	1923	0.8	0.9	1.2	1.6	13.2	115.4
12	1923	0.7	1.1	0.8	1.1	10.2	91.2
13	1923	4.6	5.6	5.7	7.8	48.1	182.9
14	1923	1.4	2.6	2.4	5.4	20.8	115.4
15	1923	2.8	4.7	4.1	5.6	30.1	142.5
16	1923	4.5	6.5	5.1	10.1	53.9	202.6
17	1923	1.8	3.5	2.5	4.8	21.9	140.8
18	1923	8.2	22.6	14.8	20.2	67.8	239.5
19	1652	5.3	15.0	7.9	11.9	33.0	158.1

2.2. Scene angular velocities velocities (LD)

		ν_{roll}		ν_{pitch}		ν_{yaw}	
ID	N	AVG	STD	AVG	STD	AVG	STD
0	1923	0.8	1.1	1.5	3.1	18.1	134.5
1	1923	1.9	3.0	4.9	8.3	23.0	146.8
2	1792	5.4	72.3	4.6	9.1	19.9	138.8
3	1923	2.6	4.2	2.6	4.3	20.3	129.2
6	1923	3.4	4.0	3.7	4.5	36.3	155.2
7	1923	3.3	5.1	5.1	8.9	48.5	206.7
8	1413	4.1	5.8	6.0	9.3	51.4	216.9
9	1923	0.9	1.7	1.6	2.0	8.6	82.2
10	1923	2.2	2.5	3.5	6.7	31.2	155.4
11	1923	1.9	3.6	3.9	10.6	19.7	115.0
11	1923	1.9	3.6	3.9	10.6	19.7	115.0
12	1923	0.5	0.9	0.6	0.7	7.0	58.1
13	1923	5.0	5.8	6.0	8.0	59.7	218.1
14	1923	2.1	5.0	2.8	5.2	29.2	153.9
15	1923	3.2	3.8	4.2	5.2	32.7	164.8
16	1923	3.8	5.7	4.0	7.7	52.1	213.6
17	1923	2.0	4.7	2.6	4.8	18.6	133.8
18	1923	7.1	9.5	12.9	19.5	67.5	216.8
19	1923	4.7	6.6	5.3	7.3	42.4	200.3

APPENDIX 3.

3.1. Spatial Frequencies (HD)

		SF_{row}		SF_{col}		SF_{rad}	
ID	N	AVG	STD	AVG	STD	AVG	STD
0	1923	0.0176	0.0064	0.0201	0.0080	0.0275	0.0079
1	1923	0.0182	0.0084	0.0202	0.0085	0.0281	0.0098
2	1923	0.0185	0.0061	0.0193	0.0076	0.0274	0.0078
3	1923	0.0200	0.0070	0.0188	0.0066	0.0280	0.0077
6	1923	0.0178	0.0064	0.0198	0.0075	0.0274	0.0077
7	1923	0.0175	0.0086	0.0226	0.0123	0.0294	0.0134
8	1717	0.0201	0.0137	0.0222	0.0149	0.0311	0.0185
9	647	0.0182	0.0043	0.0196	0.0072	0.0272	0.0067
10	1923	0.0144	0.0023	0.0147	0.0041	0.0208	0.0037
12	1923	0.0149	0.0026	0.0149	0.0043	0.0213	0.0040
13	1923	0.0186	0.0067	0.0198	0.0077	0.0278	0.0083
14	1923	0.0142	0.0022	0.0159	0.0064	0.0216	0.0057
15	1923	0.0186	0.0067	0.0199	0.0078	0.0279	0.0083
16	1923	0.0146	0.0024	0.0157	0.0055	0.0217	0.0049
17	1923	0.0182	0.0058	0.0198	0.0072	0.0275	0.0072
18	1923	0.0149	0.0038	0.0173	0.0091	0.0233	0.0087
19	1652	0.0148	0.0036	0.0164	0.0076	0.0224	0.0075
Average:		0.0171	0.0020	0.0187	0.0023	0.0259	0.0032

3.2. Spatial Frequencies (LD)

		SF_{row}		SF_{col}		SF_{rad}	
ID	N	AVG	STD	AVG	STD	AVG	STD
0	1923	0.0139	0.0013	0.0191	0.0088	0.0241	0.0077
1	1923	0.0219	0.0134	0.0291	0.0161	0.0376	0.0188
2	1792	0.0215	0.0104	0.0250	0.0126	0.0342	0.0137
3	1923	0.0205	0.0107	0.0257	0.0130	0.0340	0.0144
6	1923	0.0197	0.0102	0.0274	0.0155	0.0348	0.0164
7	1923	0.0199	0.0124	0.0300	0.0189	0.0371	0.0207
8	1413	0.0244	0.0170	0.0316	0.0200	0.0410	0.0246
9	1923	0.0138	0.0013	0.0173	0.0067	0.0225	0.0058
10	1923	0.0204	0.0110	0.0279	0.0140	0.0357	0.0155
11	1923	0.0204	0.0110	0.0279	0.0140	0.0357	0.0155
11	1923	0.0138	0.0013	0.0183	0.0079	0.0233	0.0068
12	1923	0.0204	0.0090	0.0250	0.0111	0.0333	0.0117
13	1923	0.0135	0.0013	0.0202	0.0136	0.0250	0.0123
14	1923	0.0207	0.0109	0.0278	0.0145	0.0357	0.0160
15	1923	0.0137	0.0013	0.0180	0.0087	0.0231	0.0076
16	1923	0.0201	0.0099	0.0257	0.0134	0.0338	0.0143
17	1923	0.0138	0.0013	0.0185	0.0085	0.0235	0.0074
18	1923	0.0220	0.0151	0.0298	0.0213	0.0383	0.0241
19	1923	0.0139	0.0014	0.0191	0.0096	0.0241	0.0084
Average:		0.0183	0.0036	0.0244	0.0047	0.0314	0.0062

APPENDIX 4.

4.1. Spatial velocities in radial, horizontal and vertical directions (HD)

		SV_{rad}		SV_{hor}		SV_{ver}	
ID	N	AVG	STD	AVG	STD	AVG	STD
0	1923	4.70	1.43	0.62	0.64	0.20	0.32
1	1923	4.67	1.60	0.73	0.94	0.36	0.79
2	1923	4.82	1.39	0.32	0.40	0.34	0.30
3	1923	4.52	1.53	0.89	0.96	0.61	0.41
6	1923	4.50	1.38	0.85	0.88	0.28	0.27
7	1923	3.79	2.02	1.51	1.22	0.37	1.10
8	1717	4.59	2.10	0.92	1.07	0.76	2.42
9	647	4.84	1.21	0.35	0.24	0.35	0.17
10	1923	3.71	0.72	0.17	0.21	0.20	0.14
12	1923	3.73	0.74	0.23	0.23	0.54	0.19
13	1923	4.11	1.74	1.33	1.06	0.56	0.49
14	1923	3.49	1.11	0.57	0.72	0.18	0.37
15	1923	4.62	1.42	0.85	0.82	0.39	0.55
16	1923	3.32	1.08	0.95	0.79	0.42	0.31
17	1923	4.79	1.34	0.47	0.54	0.28	0.24
18	1923	3.23	1.37	1.06	0.83	0.68	1.19
19	1652	3.58	1.09	0.65	0.60	0.45	1.14
Average:		4.18	0.56	0.73	0.36	0.41	0.17

4.2. Spatial velocities in radial, horizontal and vertical directions (LD)

		SV_{rad}		SV_{hor}		SV_{ver}	
ID	N	AVG	STD	AVG	STD	AVG	STD
0	1923	4.25	1.39	0.31	0.29	0.25	0.19
1	1923	6.50	3.22	0.56	0.84	0.45	1.14
2	1792	5.86	2.49	0.39	0.55	0.84	0.83
3	1923	5.60	2.63	0.84	1.10	0.52	0.52
6	1923	5.56	2.90	1.10	1.04	0.49	0.57
7	1923	5.19	3.36	1.53	1.44	0.67	1.66
8	1413	6.45	4.28	1.33	1.55	0.54	1.03
9	1923	3.98	1.05	0.13	0.10	0.51	0.32
10	1923	6.03	2.80	0.78	0.81	0.31	0.78
11	1923	6.05	2.79	0.62	0.78	0.66	0.96
11	1923	3.93	1.30	0.44	0.51	0.44	0.58
12	1923	5.88	2.11	0.19	0.19	0.79	0.42
13	1923	3.39	1.98	1.21	0.74	0.51	0.71
14	1923	5.98	3.01	0.74	0.94	0.32	0.41
15	1923	3.88	1.39	0.56	0.52	0.33	0.35
16	1923	5.32	2.50	0.99	1.21	0.71	0.68
17	1923	4.12	1.30	0.29	0.34	0.28	0.28
18	1923	5.06	3.38	1.72	1.70	1.15	2.41
19	1923	3.96	1.65	0.66	0.62	0.25	0.52
Average:		5.11	0.97	0.76	0.44	0.53	0.23

4.3. Spatial velocities in roll, pitch and yaw directions (HD)

		SV_{roll}		SV_{pitch}		SV_{yaw}	
ID	N	AVG	STD	AVG	STD	AVG	STD
0	1923	0.04	0.06	0.05	0.11	0.51	3.58
1	1923	0.07	0.16	0.12	0.25	0.52	3.57
2	1923	0.04	0.06	0.06	0.12	0.30	2.27
3	1923	0.08	0.13	0.06	0.13	0.51	3.18
6	1923	0.06	0.09	0.05	0.11	0.69	4.55
7	1923	0.15	0.74	0.16	0.43	0.99	4.23
8	1717	0.40	4.03	0.17	0.64	1.29	8.44
9	647	0.05	0.09	0.05	0.08	0.33	2.67
10	1923	0.02	0.02	0.02	0.02	0.20	1.85
12	1923	0.01	0.03	0.01	0.02	0.16	1.55
13	1923	0.13	0.17	0.11	0.20	0.96	4.07
14	1923	0.03	0.07	0.04	0.12	0.30	1.71
15	1923	0.08	0.15	0.08	0.14	0.58	2.86
16	1923	0.10	0.14	0.08	0.18	0.80	3.08
17	1923	0.05	0.10	0.05	0.09	0.44	3.16
18	1923	0.20	0.72	0.27	0.48	1.02	3.69
19	1652	0.14	0.69	0.15	0.41	0.54	3.03
Average:		0.10	0.09	0.09	0.06	0.60	0.31

4.4. Spatial velocities in roll, pitch and yaw directions (HD)

		SV_{roll}		SV_{pitch}		SV_{yaw}	
ID	N	AVG	STD	AVG	STD	AVG	STD
0	1923	0.02	0.03	0.03	0.06	0.25	1.83
1	1923	0.07	0.13	0.15	0.37	0.58	4.53
2	1792	0.16	1.94	0.12	0.55	0.45	4.08
3	1923	0.09	0.14	0.07	0.13	0.52	4.63
6	1923	0.12	0.16	0.10	0.16	0.80	5.10
7	1923	0.13	0.30	0.17	0.46	1.01	5.30
8	1413	0.17	0.38	0.19	0.40	1.08	5.03
9	1923	0.02	0.04	0.03	0.04	0.12	1.13
10	1923	0.08	0.10	0.10	0.21	0.76	5.57
11	1923	0.07	0.13	0.11	0.33	0.40	2.77
11	1923	0.04	0.08	0.07	0.20	0.27	1.61
12	1923	0.02	0.03	0.01	0.02	0.13	0.80
13	1923	0.13	0.17	0.13	0.22	0.80	2.92
14	1923	0.07	0.19	0.08	0.18	0.69	5.25
15	1923	0.07	0.10	0.08	0.13	0.45	2.29
16	1923	0.13	0.23	0.10	0.23	1.26	7.84
17	1923	0.05	0.13	0.05	0.12	0.26	1.87
18	1923	0.30	0.60	0.44	1.15	1.61	6.50
19	1923	0.12	0.21	0.11	0.24	0.57	2.63
Average:		0.10	0.06	0.11	0.09	0.63	0.39

APPENDIX 5.

5.1. SSQ Scores

	HD				LD			
ID	SSQ_N	SSQ_O	SSQ_D	SSQ_T	SSQ_N	SSQ_O	SSQ_D	SSQ_T
0	29	8	14	19	19	15	28	22
1	38	15	14	26	38	15	14	26
2	114	38	153	105	172	76	181	153
3	38	8	14	22	0	0	0	0
6	57	38	70	60	86	38	153	94
7	10	8	28	15	19	8	14	15
8	19	8	28	19	19	8	42	22
9	29	8	42	26	29	30	56	41
10	29	15	42	30	76	68	111	94
11	19	38	70	45	10	30	84	41
12	57	38	70	60	19	15	14	19
13	19	15	42	26	0	8	0	4
14	10	8	28	15	29	8	56	30
15	38	61	84	67	38	68	139	86
16	19	15	28	22	10	8	28	15
17	29	8	56	30	38	8	97	45
18	10	23	125	49	19	23	111	49
19	143	30	125	105	38	8	56	34

5.2. Peak FMS Scores

ID	FMS HD	FMS LD
0	5	8
1	5	5
2	11	17
3	5	0
6	7	10
7	5	5
8	3	2
9	9	4
10	4	9
11	5	4
12	12	5
13	4	1
14	0	2
15	5	6
16	3	3
17	2	2
18	1	4
19	16	6